



TITLE:

Application of High Resolution Electron-Microscopy to the Study of Carbonaceous Materials (Commemoration Issue Dedicated to Professor Eiji Suito on the Occasion of his Retirement)

AUTHOR(S):

Oberlin, A.; Boulmier, J. L.; Terriere, G. T.

CITATION:

Oberlin, A. ...[et al]. Application of High Resolution Electron-Microscopy to the Study of Carbonaceous Materials (Commemoration Issue Dedicated to Professor Eiji Suito on the Occasion of his Retirement). Bulletin of the Institute for Chemical Research, Kyoto University 1975, 53(2): 81-89

ISSUE DATE:

1975-09-25

URL:

<http://hdl.handle.net/2433/76616>

RIGHT:

Application of High Resolution Electron-Microscopy to the Study of Carbonaceous Materials

A. OBERLIN, J. L. BOULMIER, and G. TERRIERE*

Received February 26, 1975

We have used high resolution electron microscopy (dark field and lattice-fringe images) to describe short range order either in natural or synthetic chars, as well as long range order occurring during graphitization process. The chars contain stacks of 2 to 3 aromatic layers 3.4 Å to more than 8 Å apart, with diameters from 5 to 8 Å. Heat treatment leads for hard-carbons to a foam where crystallite growth is prevented by the geometry of the pore walls. On the contrary, graphitization occurs in carbons where parallel stacking is developed in large regions.

In a natural environment organic matter included in sediments is progressively degraded by the combined action of pressure and temperature established during geological times. In the same way, organic matter heat-treated until 1,000°C in the laboratory is progressively degraded too. The last limit of either experimental transformations (carbonization) or natural ones (carbonification) is an almost pure carbon solid (coke) which may eventually be progressively transformed into graphite (soft carbons) when heat-treated until 3,000°C (graphitization). Any way, most of these cokes remain very far from the crystalline state (hard carbons) even when they are heat-treated until 3,000°C.

At the beginning of their degradation, all these above defined natural or synthetic products show a very poor crystalline arrangement, the less high in carbon, the poorer the arrangement. Their X-ray diffraction study is thus difficult and lacks of precision.¹⁾ In any case, the most sophisticated crystallographic treatments only provide statistical data, corresponding to a model of average crystallite.

The main advantage of the electron microscopy towards X-ray diffraction, is an automatic performance of the Fourier synthesis usually calculated from X-ray diffraction patterns. This synthesis leads to the optical image. It is well known that the spherical aberration of the objective lens of the microscope introduces a phase shift which is very troublesome. These effects may be avoided by a separate analysis of each selectively diffracted beams *i.e* by forming a paraxial image with each of them. Every individual crystallite appears in those images as a bright dot on a dark-field. Such a dark-field image is given by the setting of an aperture in the image focal plane of the objective lens, provided this aperture being chosen as not to induce any disturbance of the image by its own diffraction figure.

Owing to these technique specially developed or elaborated in our laboratory, we have shown off the constitutive crystallites of many carbonaceous products either natural or pyrolyzed between 300 and 3000°C. We have measured the size of their crystallites

* Present address: Equipe de Recherche du C.N.R.S. n° 131, Laboratoire Marcel Mathieu, Faculté des Sciences, 45045 Orléans Cedex, France.

as well as their lattice plane spacings. We have compared the data obtained with those deduced from lattice imaging.

I) Carbonization or Carbonification Stages (% C < 100; HTT ≤ 1000°C)

Most of the carbonized or carbonified products have such a poor crystallinity that the emitted diffracted beams are very diffuse and faint. So, only two poorly contrasted diffused rings are to be observed in SAD patterns. In order to explore the whole accessible reciprocal space, we have progressively tilted the incident beam and we have formed the dark-field image for various tilting of the beam, the objective aperture remaining paraxial.²⁾ Whenever the aperture begins to intercept a diffused beam, the diffraction producing areas of the object begin to look bright on a dark field.

In our experiments we have at first used a 10 μm aperture* (half-width of the central peak of the diffraction figure smaller than 6 Å) in order to measure the crystallite sizes. As the incident beam is progressively tilted. The optical image stays uniformly dark, except for three aperture positions close to the three turbostratic carbon reflections 00.2, 10 and 11.^{3,4,5)} We have thus shown in all the chars examined, the existence of small stacks of flat parallel aromatic layers. We also deduced that the stacks are seen on their edge for the aperture first position and from the top for the two others. As an example Figs. 1 and 2 correspond to the dark-field image of a very poorly evolved natural carbonaceous material; the aperture has been centered first on 00.2, then on 10. The thickness and the diameter of the stacks have been measured from such pictures of various samples. In any case, even in soft carbons precursors, the average thickness and diameter have been found less than 10 Å (two aromatic layers and less than ten aromatic cycles).

In the dark-field image, a given crystallite lights-up at its maximum of intensity when the aperture is exactly adjusted on one of its diffused beam, which means that the aperture is set at a distance $L\lambda/d_{hkl}$ of the incident beam ($L\lambda$ is the diffraction constant of the microscope and d_{hkl} is the spacing of the (hkl) lattice planes). This fact gives us the opportunity to measure the d spacing of an individual crystallite as small as 10 Å. In order to measure precisely the value of d_{hkl} , we use a photographic process. After each picture taken for a given tilting of the incident beam, we have superimposed on a second picture the contour of the selected objective aperture upon the SAD pattern, finally we have taken a third picture of internal standard which allows the measure of $L\lambda$. We thus know the value of $L\lambda/d_{hkl}$ which corresponds to the aperture center (5, 6). The error depends on the aperture diameter. Consequently, the smallest aperture has to be selected and we have chosen a 5 μm one (0.1 Å⁻¹). In order to test the method we have measured fifty times the graphite $d_{00.2}$ ($d_{00.2}=3.354$ Å) and we found $3.3 \text{ Å} < d < 3.5 \text{ Å}$. We have thus kept this experimental range for all the examined samples.

We firstly applied the above technique to natural samples (kerogens) containing about 75% of carbon. The first bright dots appear for an aperture position slightly before 0.13 Å^{-1} ($d=8 \text{ Å}$). They light off when the aperture intercepts higher values in the reciprocal space. They are replaced by other dots which in turn light off. The last dots to light on correspond to 0.32 Å^{-1} ($d=3.1 \text{ Å}$). After having applied the cor-

* in our conditions, this corresponds to a diameter of $|\vec{s}| = \frac{2 \sin \theta}{\lambda} = 0.2 \text{ Å}^{-1}$

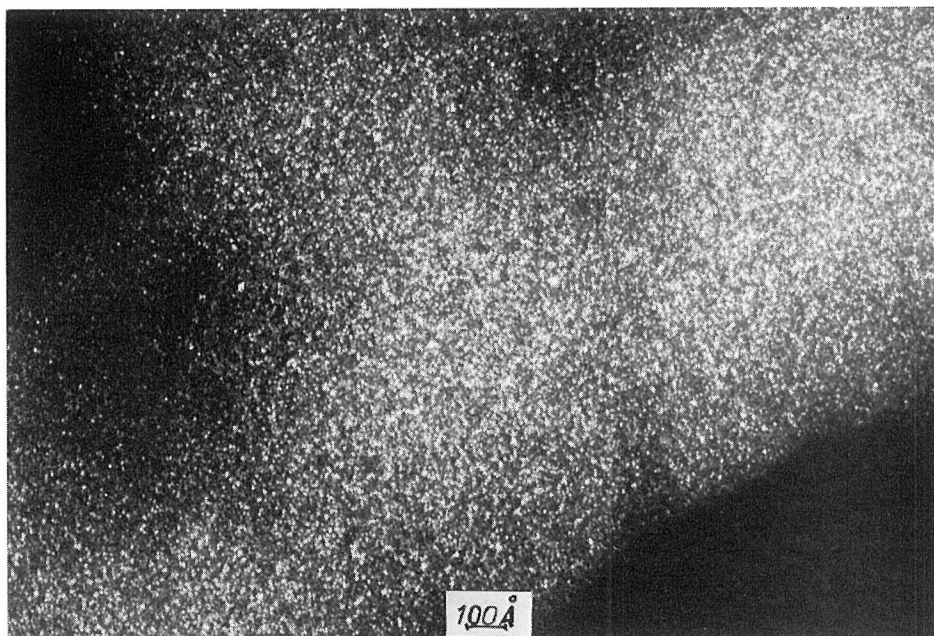


Fig. 1. Natural sample heat-treated at 300°C; 00.2 dark-field; $\times 500,000$

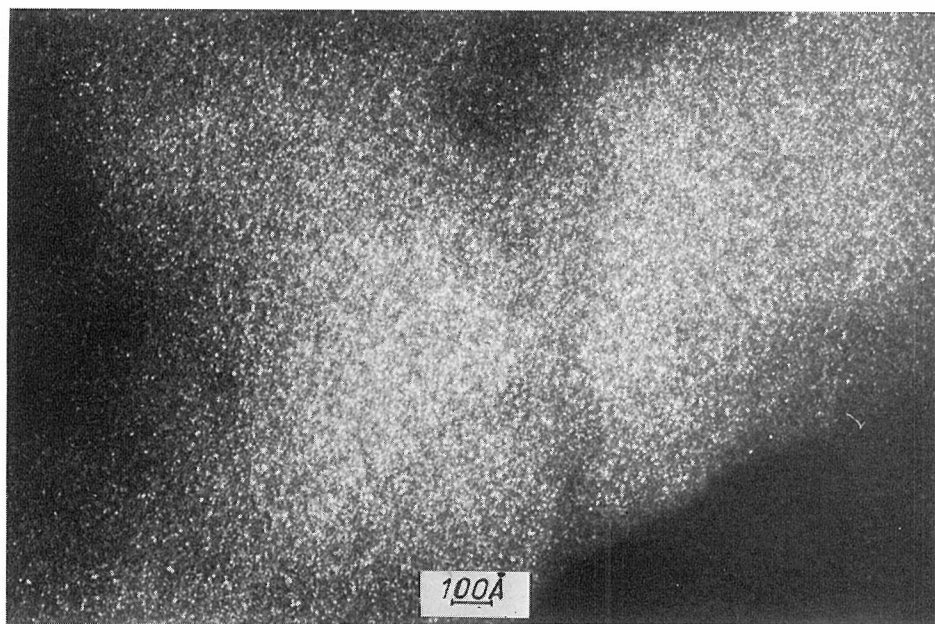


Fig. 2. Same sample as Fig. 1; 10 dark-field; $\times 500,000$

rection of the extension of the 00.2 reciprocal spike, this value reaches $3,4 \text{ \AA}$ which is the minimum normal value for turbostratic carbons. Beyond $0,32 \text{ \AA}^{-1}$ the optical image becomes entirely dark. Most of the spots lit up at their maximum are located between $0,20$ and $0,25 \text{ \AA}^{-1}$, which corresponds to a $4\text{--}5 \text{ \AA}$ average value for the interlayer spacing. These data have to be interpreted as resulting from a variation of the distance between the carbon layers of the various stacks constituting the sample. The shifting of the objective aperture describes the histogram of the d spacing frequency. This phenomenon of interlayer spacing spreading progressively lessens as carbonization or carbonification increases and is minimum in the case of soft carbon precursors⁵). It may, however, be perceived even in almost pure carbon samples heat-treated at 1000°C .

From the dark-field pictures we may determine whether or not some preferred orientation exists in the sample, *i.e.* whether or not the carbon layers of two neighbouring stacks are more or less parallel to each other (*loc cit* 3,4,5). An \vec{a} axis and a \vec{c} axis may be defined for each stack, by analogy with graphite. 00.2 dark-field pictures would give informations about the \vec{c} axis preferred orientation and the 10 or 11 dark-field pictures would describe the \vec{a} axis preferred orientation, if any. If neither \vec{a} or \vec{c} axis happen to be parallel to some others, the bright dots would appear uniformly distributed in the particles, in any position of the objective aperture on the Debye-Scherrer ring. Figures 1 and 2 for instance illustrate this case respectively for 00.2 and 10, *i.e.* for \vec{c} and \vec{a} axis. When some \vec{a} or \vec{c} axis becomes locally roughly parallel, the bright dots would associate into clusters; these clusters will appear whenever the aperture intercepts their common diffracted beam. Figure 3 is a dark-field picture using 00.2 beam, in the case of a highly carbonified natural sample. The carbonification process of these materials is characterized by a progressive increase of the cluster size (these clusters of bright dots are the areas where \vec{c} axis are roughly parallel) except for soft carbons precursors. Those latter ones go through a liquid stage at the very beginning of the carbonization process ($400\text{--}500^\circ\text{C}$)

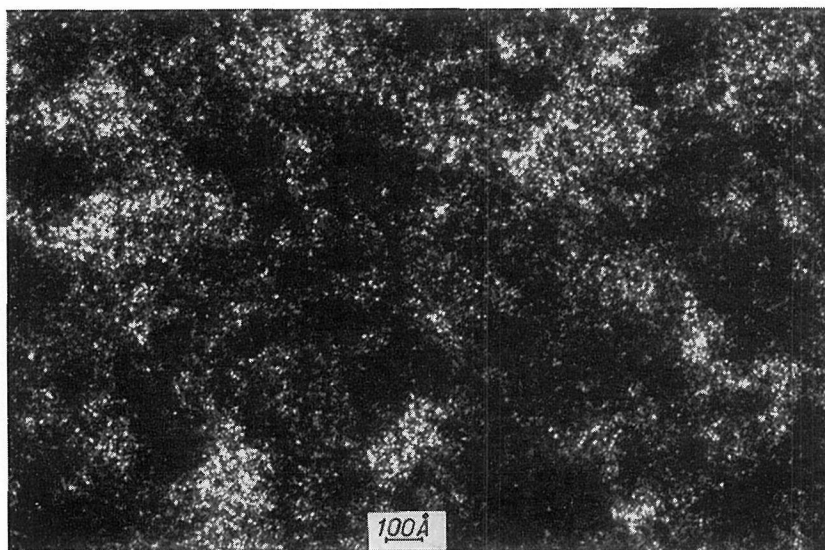


Fig. 3. Same sample as in Fig. 1 heat-treated at 600°C ; 00.2 dark-field; $\times 500,000$

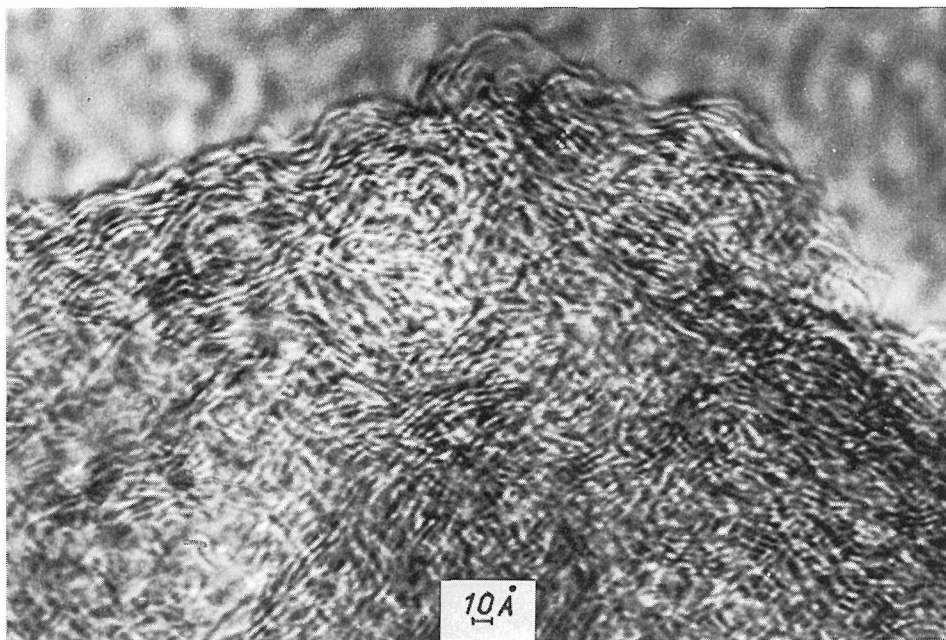


Fig. 4. Hard carbon heat-treated at 1000°C; lattice imaging; $\times 2,600,000$

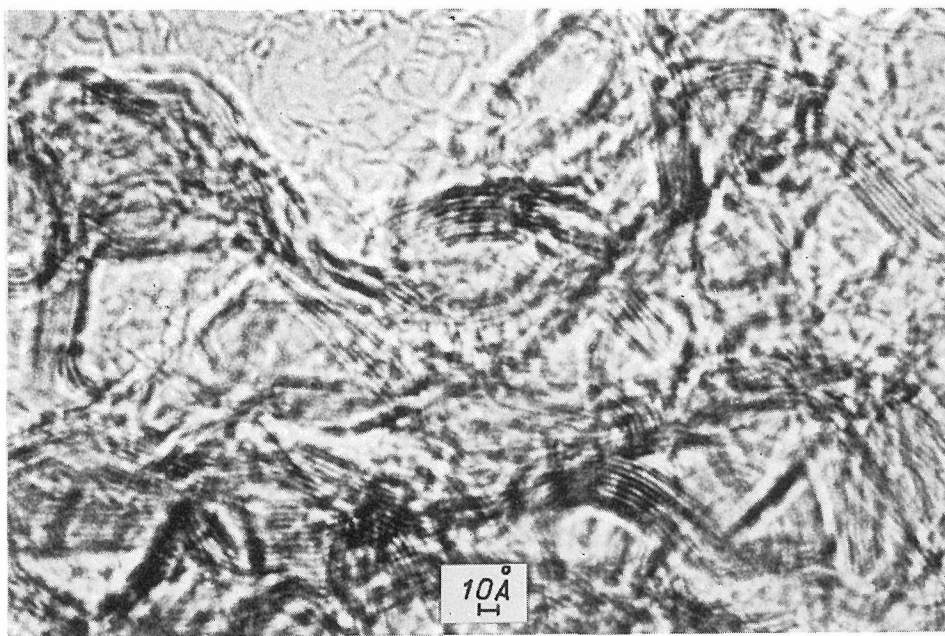


Fig. 5. Hard carbon heat-treated at 2700°C; lattice imaging; $\times 2,600,000$

and then through a new phase, the mesophase.⁷⁾ When observed in polarized light with an optical microscope, the spherical particles of mesophase appear anisotropic. They contain aromatic macromolecules in strong parallel preferred orientation in areas as large as the particles themselves (a few microns). If we compare the size of the areas where the carbon layers are parallel in soft carbon precursors and in hard carbon precursors, we see a striking difference: the latter ones always are smaller than 200–300 Å.

The possible development of an \vec{a} axis preferred orientation has been followed by 10 dark-field micrographs and we have found that none is observable before heat-treatment temperatures higher than 1000°C.

From all the previous data, a char (either natural or synthetic) can be described as made of small carbon layers piled up by two and less than 10 cycles in size; their interlayer spacing broadly varies inside a given sample. In the bulk, these small stacks either are nearly random (hard carbon precursors) or present a strong parallel preferred orientation (soft carbon precursors). During heat-treatment process, some stacks of hard carbon precursors associate and acquire a roughly parallel preferred orientation in small areas; their interlayer spacing spreading progressively decreases but it does not appear any preferred orientation of the \vec{a} axis. The soft carbon precursors are made of the same elementary "bricks" but show a very narrow interlayer spacing spreading, as well as a nearly perfect preferred parallel orientation developed in large areas. Figures 4 and 6 show lattice imaging pictures using the 00.2 reflection and the incident beam respectively for a hard carbon sample and for a soft carbon one, which illustrate quite well the above data.

II) Graphitization Range ($\text{HTT} \leq 2900^\circ\text{C}$)

As far as this range is concerned, our knowledge only comes from experimental

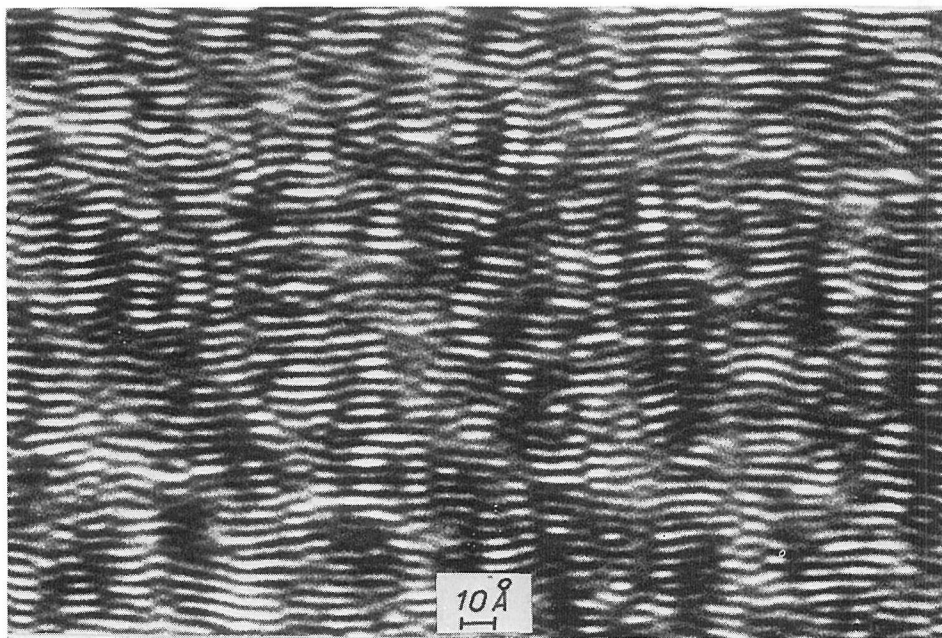


Fig. 6. Graphitizable carbon heat-treated at 900°C; lattice imaging; $\times 4,500,000$

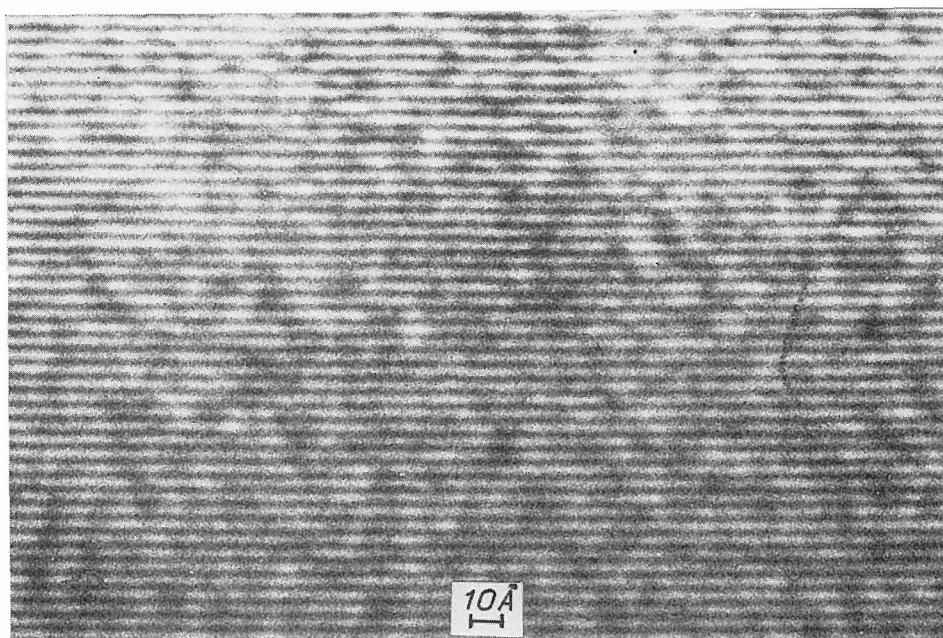


Fig. 7. Graphitizable carbon heat-treated at 2900°C; lattice imaging; $\times 4,500,000$

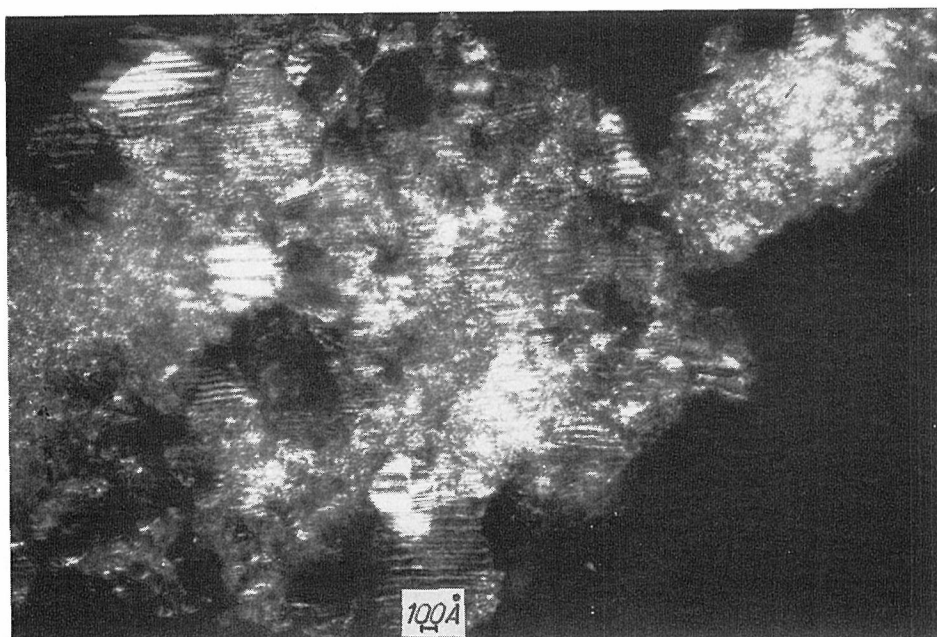


Fig. 8. Hard carbon heat-treated at 2700°C; 11 dark-field; $\times 200,000$

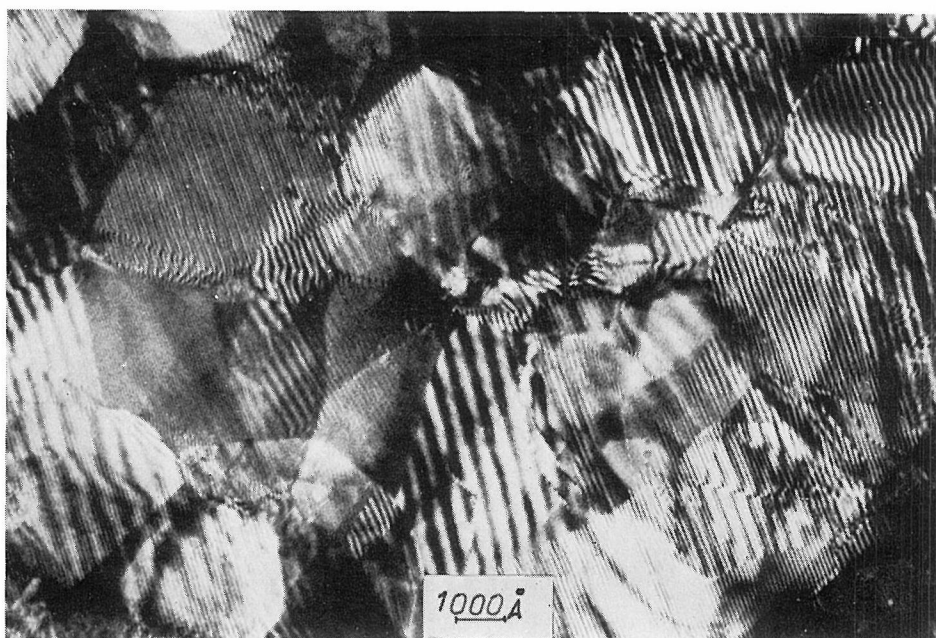


Fig. 9. Graphitizable carbon heat-treated at 2900°C; 10 dark-field; $\times 65,000$

work, since until now no natural samples have been found to present either hard or soft carbon behavior. Samples of both categories heat-treated at various temperature ranging from 1000°C to 2900°C have been compared, in using either dark-field pictures or lattice imaging (loc cit 5). Non graphitizable carbons present a very porous structure, comparable to a foam where carbon layers form the walls of the pores, as shown in lattice imaging (Fig. 5). The crystallite growth is consequently prevented by the geometry of the sample and such a carbon cannot graphitize. For the highest HTT, the diameter of the crystallites given by 11 dark-field pictures (Fig. 8) is about 100 Å in size. On the contrary, Fig. 7 (lattice imaging) and Fig. 9 (10 dark-field picture) show that large flat unconstrained layers may be produced in soft carbons. The graphitization process is greatly facilitated by the existing strong preferred orientation of the \vec{c} axis. The less than 10 Å bright dots previously noticed in dark-field are replaced by large monocrystalline areas more than 3000 Å wide, which present moires fringes. Both dark-field analysis and lattice imaging well agree, as far as study of poorly crystallized materials and study of crystal growth are concerned. Therefrom, each individual crystallite may be shown, and its size measured as well as its d spacing. Occurrence of some parallel orientation of the crystallite \vec{a} or \vec{c} axis may be determined in the same way.

REFERENCES

- (1) J. Mering and A. Oberlin, "The electron optical investigations of clays," Mineralogical Soc, London, (1971), p. 197.
- (2) A. Oberlin and G. Terriere, *J. Microscopie*, **14**, 1 (1972).
- (3) A. Oberlin, J. L. Boulmier, and B. Durand, *Adv. Organ. Geochem.*, **15**, (1973).

High Resolution Electron-Microscopy of Carbonaceous Materials

- (4) A. Oberlin, J. L. Boulmier, and B. Durand, *Geochim. Cosmochim. Acta*, **38**, 647 (1974).
- (5) A. Oberlin, G. Terriere, and J. L. Boulmier, *Tanso*, **80**, 29 (1975).
- (6) A. Oberlin, G. Terriere, and J. L. Boulmier, *J. Microscopie*, **21**, 301 (1975).
- (7) J. D. Brooks and G. Taylor, "Chemistry and Physics of Carbon," Marcel Dekker, N.Y., (1968),
p. 4